An Ultra-Sensitivity Cancellation Type Sensor Based on Microstrip Meander-Line

2021 IEEE 3rd International Conference on Circuits and Systems (ICCS) | 978-1-6654-1234-6/21/$31.00 ©2021 IEEE | DOI: 10.1109/ICCS52645.2021.9697208

Xiaoqin Liu
School of Aeronautics and Astronautics
University of Electronic Science and Technology of China
Chengdu, China
xqliu@std.uestc.edu.cn

Huan Zou
School of Aeronautics and Astronautics
University of Electronic Science and Technology of China，
Aircraft Swarm Intelligent Sensing and Cooperative Control Key Laboratory of Sichuan Province
Chengdu, China
hzou82@uestc.edu.cn

Bo Zhu
School of Aeronautics and Astronautics
University of Electronic Science and Technology of China
Chengdu, China
zhubo@std.uestc.edu.cn

Hui Lin
School of Aeronautics and Astronautics
University of Electronic Science and Technology of China
Chengdu, China
LINHUI_546484@163.com

Haiyang Wang
School of Electronic Science and Engineering (National Exemplary school of Microelectronics)
University of Electronic Science and Technology of China
Chengdu, China
hhywa@uestc.edu.cn

***Abstract*—The analysis of dielectric properties in Novel Coronavirus （COVID-19） has become an important research branch since the outbreak of the epidemic in 2019. In order to detect the dielectric properties of microfluidics like virus with higher sensitivity, a radio frequency sensor model is proposed in this paper. First, based on the excellent characteristics of the microstrip meander-line such as more concentrated electric field distribution, the microstrip meander-line is introduced into the design of traditional cancellation sensor, which is called the meander sensor. Then, the relationship between transmission coefficients of the system and dielectric properties of microfluidics is given in this paper. The simulation results verify the ultra-sensitivity of the meander sensor. Even though the relative permittivity of microfluidics is changed in the order of magnitude 10^{-2}, the measurement results of the meander sensor also change significantly. However, the straight sensor can only measure changes of relative permittivity in the order of magnitude 10^{-1}. What's more, there is a more concentrated measurement range for the meander sensor. This will be more practical for measuring weak changes of dielectric properties caused by the microfluidics itself and its interactions.**

Keywords—microfluidics, microstrip meander-line, permittivity, radio frequency sensor, ultra-sensitivity

I. INTRODUCTION

There is a wide applications for dielectric properties measurement of microfluidics in biology, including studies of irreversible electroporation irreversibly destroying cells of target tissues [1], the relationship between temperature and hematocrit value [2], and the changes in bacterial biomass and growth stage [3]. During the period of the Novel Coronavirus Disease (COVID-19) pandemic, it has become one of the research hotspots to use biosensors to quickly detect the electrical properties of Novel Coronavirus and its products [4]-[6]. At present, in the biomedical research, the basic principle of dielectric properties measurement based on planar transmission line method is to directly extract the change information of transmission and reflection coefficients (including amplitude and phase) of microwave transmission line. However, there is an inherent defect in this method, which is that the sensitivity of the system will be seriously affected when directly extracting weak changes from strong background signals. When the size of the measured subjects is extremely small (micron or nanometer) such as cells or viruses, this sensitivity problem becomes more serious. To solve this problem, a planar cancellation type structure is proposed in [7]-[9], which could effectively extract weak changes of dielectric properties of microfluidics by offsetting strong background signals. Subsequently, many improvements based on the planar cancellation type sensors have been proposed. Based on coplanar waveguide structure, an ultra-sensitive radio frequency sensor was proposed to measure yeast cells in [10]. And after further improvement, the transmission coefficient S_{21} reached -70 dB by calibration with deionized water in [11]. Then this sensor was used to measure the molarity of primary alcohol and the lowest limit is 0.25%.

However, all these traditional cancellation type sensors are designed based on planar straight microstrip lines (Straight Sensor), and their sensitivity is limited. The meander transmission lines are most studied as microstrip meander-line slow-wave structure, which mainly consist of periodic arrangements of meander microstrip lines. According to previous studies [12], [13], in the analysis of the field distribution of the microstrip meander-line, the electromagnetic signal is amplified in the meander part because of the interaction between the sheet electron beam and slow wave. Therefore, in order to improve the sensitivity of traditional cancellation type sensor, the microstrip meander-line is introduced into this kind

Supported by National Natural Science Foundation of China. (61671132, 61601086)

of sensor (Meander Sensor). Compared with the straight sensor, the measuring sensitivity is improved effectively and the measuring range is more concentrated by deploying the meander sensor. For ultrafine microfluidics, it is exceedingly practical for the analysis of dielectric properties changes of it, because this measurement does not require too wide measurement range, but requires high measurement sensitivity [14].

The rest of this paper is organized as follows: In Section II, the measurement principle of meander sensor is introduced. Then the comparative analysis of meander sensor and straight sensor is presented in Section III. Finally, the main conclusions are drawn in Section IV.

II. The Measurement Principle of Meander Sensor

The schematic diagram of the cancellation type sensor based on microstrip meander-line is shown in Fig. 1. The input port of the signal is Port1 and the output port is Port2. The sensor is mainly composed of two identical Wilkinson power dividers, a meander line branch, and a straight line branch. Compared with the traditional straight sensor, the upper test branch of the meander sensor is changed to the microstrip meander-line with the length of λ/2 (which can also be an odd multiple of λ/2). The relationship between transmission coefficients of the system and dielectric properties of microfluidics will be discussed below.

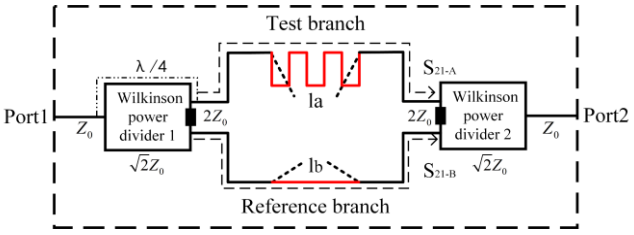

Fig. 1. The schematic diagram of the cancellation type sensor based on microstrip meander-line

Assuming that the path length from the output of the first Wilkinson power divider to the left of the test branch is l . l_a is the length of the meander test branch and l_b is the length of the straight reference branch. The difference between l_a and l_b is odd times of half-wavelength

$$l_a - l_b = n\frac{\lambda}{2}(n = 1,3,5\cdots). \tag{1}$$

S_{21_A} and S_{21_B} stand for the signal transmission coefficients of the upper and lower branches, respectively. The signal transmission coefficients from port 1 to port 2 can be expressed as

$$S_{21} = S_{21\_A} + S_{21\_B}. \tag{2}$$

Then, S_{21_a} and S_{21_b} represent the transmission coefficients of the l_a and l_b segments, respectively. Whereas S_{21_sa} and S_{21_sb} are the transmission coefficients of the signal lines of the l_a and l_b segments when there are not microfluidics in l_a and l_b segments. Where S_{21_MUT} and S_{21_REF} indicate the transmission coefficients of the materials under test (MUT) and reference (REF). S_{21_Ea} and S_{21_Eb} represent the transmission coefficients of the remaining signal lines after removing l_a section in the upper branch and removing l_b section in the lower branch. Equation (2) can be rewritten to

$$\begin{aligned} S_{21} &= S_{21\_Ea} \times S_{21\_Sa} \times S_{21\_MUT} \\ &+ S_{21\_Eb} \times S_{21\_Sb} \times S_{21\_REF.} \end{aligned} \tag{3}$$

For the transmission coefficient S_{21_a} and S_{21_b}, there are [15]

$$S_{21\_a} = \frac{2Z_0}{2Z_0 + Z_a(\omega)} \tag{4}$$

where Z_0 is the characteristic impedance, and the impedance of the meander test branch can be expressed as $[Z_a(\omega)]^{-1} = G_a(\omega) = j\omega C_p + j\omega C_l \varepsilon_a$ where ε_a is the complex permittivity of the microfluidics placed in the l_a section. C_p is the parasitic capacitance and C_l is the liquid channel capacitance. C_l will change with the changes of liquid type and volume in two branches. We use ΔS_{21_MUT} to represent the difference value of transmission coefficients between the upper branch and the lower branch when there are different microfluidics in two branches, then

$$S_{21\_a} = S_{21\_Sa} \times S_{21\_REF} + \Delta S_{21\_MUT.} \tag{5}$$

1) When the same microfluidics are added to the test branch and the reference branch, $S_{21\_MUT} = S_{21\_REF}$, and $\Delta S_{21\_MUT} = 0$. Assuming that there is no loss on the transmission line, (3) can be written as [16]

$$\begin{aligned} S_{21} &= S_{21\_Ea} \times (S_{21\_Sa} \times S_{21\_REF}) \\ &+ S_{21\_Eb} \times (S_{21\_Sb} \times S_{21\_REF}) \\ &= e^{-\gamma(l_b + n\frac{\lambda}{2} + 2l)} \times S_{21\_REF} + e^{-\gamma(l_b + 2l)} \times S_{21\_REF} \\ &= 0. \end{aligned} \tag{6}$$

The cancellation type sensor can offset the background noise and eliminate the parasitic effect, which can solve the traditional problem that it is hard to directly extract the weak changes information from strong background signals.

2) When the microfluidics added in the test branch and the reference branch are different, $S_{21\_MUT} \neq S_{21\_REF}$, and $\Delta S_{21\_MUT} \neq 0$, then

$$\begin{aligned} S_{21} &= S_{21\_Ea} \times (S_{21\_Sa} \times S_{21\_REF} + \Delta S_{21\_MUT}) \\ &+ S_{21\_Eb} \times (S_{21\_Sb} \times S_{21\_REF}) \\ &= S_{21\_Ea} \times \Delta S_{21\_MUT} \\ &= S_{21\_Ea} \times \left[\frac{2Z_0}{2Z_0 + Z_a(\omega)} - \frac{2Z_0}{2Z_0 + Z_b(\omega)} \right] \\ &= P(\varepsilon_a - \varepsilon_b). \end{aligned} \tag{7}$$

where $S_{21\_Ea} \times S_{21\_Sa} \times S_{21\_REF} + S_{21\_Eb} \times S_{21\_Sb} \times S_{21\_REF} = 0$, ε_a and ε_b stand for the complex permittivity of the microfluidics added at the test branch l_a and the reference branch l_b . When $S_{21\_MUT} \neq S_{21\_REF}$, the difference of the complex permittivity between the test branch and the reference branch is directly related to the transmission coefficient S_{21} measured by the system. It will be another interesting reaserch direction to replace the microstrip line in Fig. 1 with coplanar waveguide structure [17] with better performance.

III. Comparative Analysis of Meander Sensor and Straight Sensor

This sensor uses Rogers 6010 board with the relative permittivity of 10.2, the dielectric thickness of 0.635 mm, and the metal thickness of 18μm. The operating frequency of the sensor is 10GHz. When there is no load, both meander and straight sensors cannot be used directly to measure the changes of permittivity of microfluidics before calibration with the same microfluidics. The unknown parameter P in (7) can be confirmed by calibration. At the same time, we can compensate attenuation and fine-tune the electrical length of the two branches to acquire better offset performance. In this paper, deionized water (the relative permittivity is 81 and the conductivity is 0.0002 S/m) is used as the calibration solution. The same volume (1.88 mm × 2.13 mm × 0.1 mm = 0.40044 $mm^3 \approx 400$ nl) of deionized water was placed in the test and reference areas of the meander and straight sensors, respectively. In order to analyze and compare reasonably the data later, the S_{21} parameters of the two sensors are calibrated to similar positions. The simulation results of the calibration model and scattering parameters are shown in Fig. 2. The orange areas in (a) and (b) indicate the calibration solution of deionized water. From (c) and (d), the S_{21} of the calibrated meander sensor can reach -91.57 dB at 10.09 GHz, and the S_{21} of the calibrated straight sensor can reach -95.80 dB at 10.19 GHz, which indicate that the two sensors achieve a good offset effect when their upper and lower branches are placed the same calibration solution.

A. Sensitivity Analysis of Sensors

The two sensors can measure the changes of permittivity of microfluidics after calibration. At first, dielectric properties (relative permittivity and conductivity) of microfluidics in the reference area are not changed. Then the relative permittivity of microfluidics in the test area is changed, but the conductivity is not changed. The changes of permittivity are 0.1, 0.01, and 0.001, respectively. Because the variation is particularly weak in natural environment when the amount of virus itself and its products is small [14]. The changes of S_{21} value of two sensors are observed to study their sensitivity in measuring the changes of relative permittivity. The measurement results of the meander sensor are shown in Fig. 3. As can be seen from the test results above, the meander sensor can measure changes of relative permittivity on the order of at least 10^{-2}, which can detect the relative change of 0.01%. When measuring a change of 0.001 (the relative permittivity of the microfluidics in the test area is set to 80.999), the value of S_{21} remains virtually unchanged compared with the original value that is calibrated with deionized water.

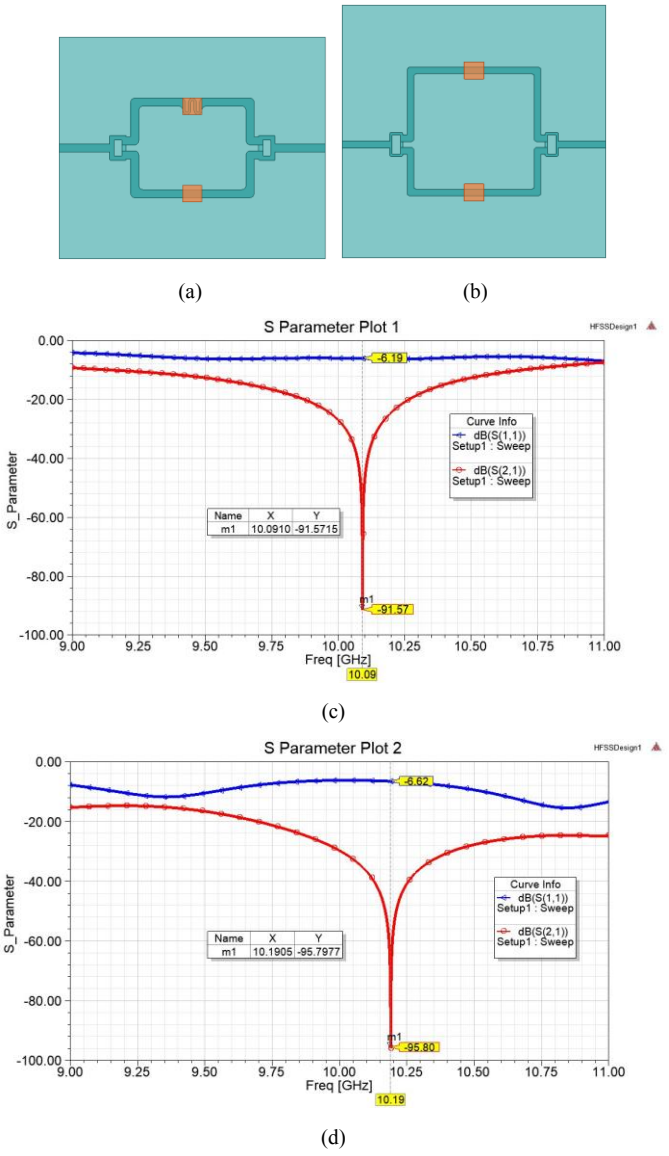

Fig. 2. The calibration model and scattering parameters of meander and straight sensors. (a)The calibration model of meander sensor. (b) The calibration model of straight sensor. (c)The scattering parameters of meander sensor. (d)The scattering parameters of straight sensor.

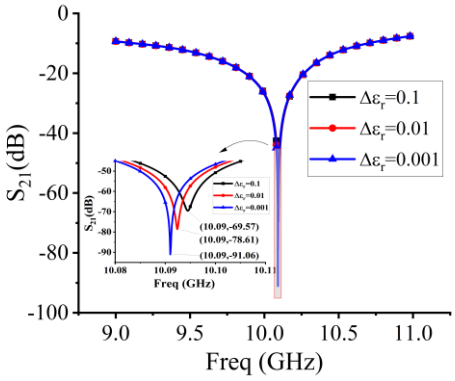

Fig. 3. The transmission coefficients S_{21} of the meander sensor vary with different order of magnitude changes of relative permittivity.

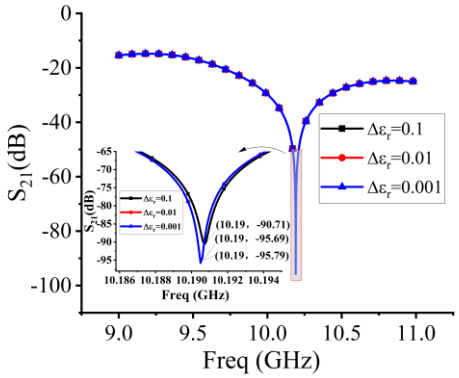

Fig. 4. The transmission coefficients S_{21} of the straight sensor vary with different order of magnitude changes of relative permittivity.

The same simulation procedure is used to explore the sensitivity of the straight sensor in measuring the changes of relative permittivity. The measurement results are shown in Fig. 4. The straight sensor can measure the changes of relative permittivity on the order of at least 10^{-1}. When changes of 0.01 and 0.001 are measured, the value of S_{21} remains almost unchanged compared with the original value (shown in Fig. 4 as the red and blue lines almost overlap).

TABLE I. COMPARISON OF S_{21} CHANGES OF TWO SENSORS

$\Delta\varepsilon_r$	10^{-1}	10^{-2}	10^{-3}
$\lvert\Delta S_{21}\rvert$ (dB) (meander sensor)	22.00	12.96	0.51
$\lvert\Delta S_{21}\rvert$ (dB) (straight sensor)	5.09	0.11	0.01
$\Delta\lvert\Delta S_{21}\rvert$ (dB)	16.91	12.85	0.50

A further tabular comparison of the S_{21} parameter changes caused by the meander and straight sensors is shown in Table I. Compared with the simulation results of the two sensors, the meander sensor can detect the changes of relative permittivity on the order of 10^{-2}. The S_{21} parameter changes measured by the meander sensor is 16.91 dB higher than that of the straight sensor even on the same order of magnitude ($\Delta\varepsilon_r = 0.1$). In other words, the sensor that includes the microstrip meander-line slow-wave structure can improve sensitivity of traditional cancellation type sensor.

B. Analysis of Measuring Range of Sensors

From the above analysis, it can be concluded that the measuring sensitivity of the meander sensor is higher than the straight sensor. But does the meander sensor maintain the same measurement range as the straight sensor while improving the sensitivity? Therefore, in this subchapter, we will only change the relative permittivity of microfluidics in the test area in a wide range to explore the measurement range of the meander sensor and compare it with the straight sensor . The simulation results of the meander sensor are shown in Fig. 5. The frequency and amplitude of S_{21} change only within a certain range ($\Delta\varepsilon_r \le 11$) as the relative permittivity changes. The S_{21} amplitude changes are small outside the range.

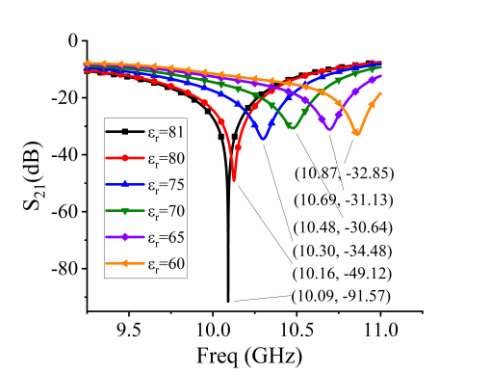

Fig. 5. The changes of transmission coefficients S_{21} of meander sensor with the changes of relative permittivity.

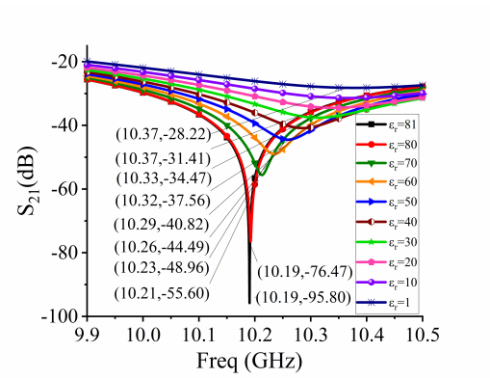

Fig. 6. The changes of transmission coefficients S_{21} of straight sensor with the changes of relative permittivity.

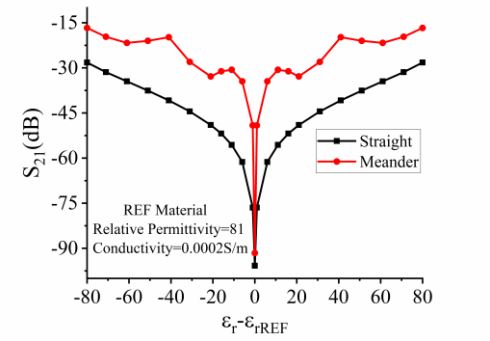

Fig. 7. The transmission coefficients S_{21} of two sensors at different relative permittivity.

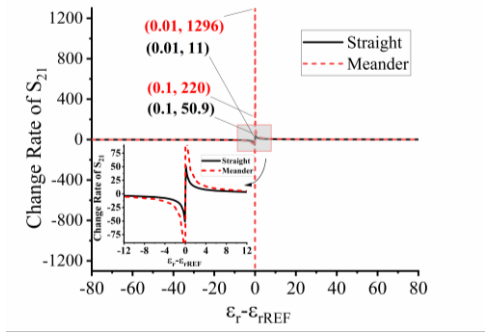

Fig. 8. The change rate of S_{21} parameters of two sensors.

The same method is used to simulate and analyze the changes of transmission coefficients S_{21} caused by different relative permittivity for the straight sensor, and the simulation results are shown in Fig. 6. The frequency and amplitude of S_{21} change regularly in the whole range ($1 \le \varepsilon_r \le 81$) as the relative permittivity changes. There is a more concentrated measurement range for the meander sensor. To further compare the measuring range of the meander and straight sensors, the measurement results of two sensors are plotted into the same graph, as in Fig. 7. When the straight sensor measures the changes of relative permittivity, the S_{21} parameter can vary regularly throughout the range ($|\Delta\varepsilon_r| \le 80$). Whereas the meander sensor can only vary regularly in the range ($|\Delta\varepsilon_r| \le 11$). Because there is a reverse folding point when $\Delta\varepsilon_r = 11$. The measurement cannot be made beyond this range, otherwise errors will occur. In other words, the meander sensor increases the measurement sensitivity while concentrating the measurement range, making the measurement more focused.

The change rate of S_{21} parameter is defined as follows

$$Change\ Rate\ of\ S_{21} = \frac{\Delta S_{21}}{\Delta\varepsilon}. \quad (8)$$

The data from the above simulation is further plotted as the change rate of S_{21} parameters in Fig. 8. Both meander and straight sensors are more sensitive in measuring very small changes of relative permittivity. However, compared with the straight sensor, the meander sensor has higher measuring sensitivity and more concentrated measuring range, which is better for measuring small changes of the microfluidics.

IV. Conclusion

In order to improve the sensitivity of cancellation type sensor and detect the changes of dielectric properties caused by the microfluidics itself and its interactions, we proposed a novel sensor with higher sensitivity based on microstrip meander-line. Microstrip meander-line with more concentrated field distribution in the meander part is introduced into the design of traditional cancellation type sensor. The results show that the meander sensor can detect the changes of relative permittivity in order of magnitude 10^{-2} and the maximum change rate of S_{21} parameters can reach 1296. The change rate of S_{21} parameters improves 100 times compared with the maximum in [15]. The meander sensor does improve the measuring sensitivity, and concentrate the measuring range at the same time, which is of great significance for the detection of virus properties.

In next work, a real sensor will be produced and tested with suitable microfluidics to verify above simulation results. At the same time, an adjustable cavity can be designed to shield the interference of the environment and compensate the loss from long transmission lines, which will make the sensor to acquire more stable results and higher sensitivity.

Acknowledgment

This work is supported by the National Natural Science Foundation of China (61671132, 61601086).

References

[1] R. E. Neal, P. A. Garcia, J. L. Robertson, and R. V. Davalos, "Experimental characterization and numerical modeling of tissue electrical conductivity during pulsed electric fields for irreversible electroporation treatment planning," IEEE Trans. Biomed. Eng., vol. 59, no. 4, pp. 1076-1085, Apr 2012.

[2] M. Wolf, R. Gulich, P. Lunkenheimer, and A. Loidl, "Broadband dielectric spectroscopy on human blood," Bba-gen. Subjects, vol. 1810, no. 8, pp. 727-740, Aug 2011.

[3] C. Zhang, A. Revil, Y. Fujita, J. Munakata-Marr, and G. Redden, "Quadrature conductivity: A quantitative indicator of bacterial abundance in porous media," Geophysics, vol. 79, no. 6, pp. D363-D375, Nov-Dec 2014.

[4] B. Mojsoska, S. Larsen, D. A. Olsen, J. S. Madsen, I. Brandslund, and F. A. Alatraktchi, "Rapid sars-cov-2 detection using electrochemical immunosensor," Sensors, vol. 21, no. 2, pp. 11, Jan 2021.

[5] M. Alafeef, K. Dighe, P. Moitra, and D. Pan, "Rapid, ultrasensitive, and quantitative detection of sars-cov-2 using antisense oligonucleotides directed electrochemical biosensor chip," ACS Nano, vol. 14, no. 12, pp. 17028-17045, Dec 2020.

[6] E. Cesewski and B. N. Johnson, "Electrochemical biosensors for pathogen detection," Biosens. Bioelectron, Review vol. 159, pp. 29, Jul 2020.

[7] C. R. Song, P. S. Wang, and Ieee, "On-chip cancellation of parasitic effects for dielectric permittivity measurement," in 2008 ieee mtt-s international microwave symposium digest, vols 1-4, (Ieee mtt-s international microwave symposium. New York: Ieee, 2008, pp. 1720-1723.

[8] H. Q. Zhang, C. R. Song, and P. S. Wang, "A new method for high-frequency characterization of patterned ferromagnetic thin films," J. Appl. Phys., Proceedings Paper vol. 105, no. 7, pp. 3, Apr 2009.

[9] C. R. Song and P. S. Wang, "A radio frequency device for measurement of minute dielectric property changes in microfluidic channels," Appl. Phys. Lett., vol. 94, no. 2, pp. 3, Jan 2009.

[10] Y. Yang et al., "Distinguishing the viability of a single yeast cell with an ultra-sensitive radio frequency sensor," Lab Chip, vol. 10, no. 5, pp. 553-555, 2010.

[11] W. N. Liu, Y. Yang, and K. M. Huang, "A radio frequency sensor for measurement of small dielectric property changes," J. Electromagnet Wave, vol. 26, no. 8-9, pp. 1180-1191, 2012.

[12] F. Shen et al., "A novel v-shaped microstrip meander-line slow-wave structure for w-band mmpm," IEEE Trans. Plasma Sci., vol. 40, no. 2, pp. 463-469, Feb 2012.

[13] S. Sengele, H. R. Jiang, J. H. Booske, C. L. Kory, D. W. van der Weide, and R. L. Ives, "Microfabrication and characterization of a selectively metallized w-band meander-line twt circuit," IEEE Trans. Electron Devices, vol. 56, no. 5, pp. 730-737, May 2009.

[14] M. P. Hughes, H. Morgan, and F. J. Rixon, "Measuring the dielectric properties of herpes simplex virus type 1 virions with dielectrophoresis," Biochimica et Biophysica Acta (BBA) - General Subjects, vol. 1571, no. 1, pp. 1-8, 2002/05/10/ 2002.

[15] W. N. Liu, "A novel technology for measurements of dielectric properties of extremely small volumes of liquids," Int. J. Antenn. Propag, vol. 2016, pp. 5, 2016.

[16] H. Y. Wang, X. Q. Liu, R. Xiong, and H. Zou, "Adjustable cancellation type high sensitivity radio frequency sensor," Measurement, vol. 168, pp. 6, Jan 2021.

[17] H. O. Issa, W. S. Diab, and M. W Wehbi, "A Compact X-Band Coplanar Waveguide Hybrid Lowpass Filter," IJEETC, vol. 9, pp. 105, March 2020.